3

LIFT Using a Dynamic Release Layer

Alexandra Palla Papavlu [1,2] and Thomas Lippert [1,3]

[1] Paul Scherrer Institute, Research with Neutrons and Muons Division, 5232 Villigen, Switzerland
[2] National Institute for Lasers, Plasma and Radiation Physics, Atomistilor 409, 077125 Magurele, Romania
[3] ETH Zürich, Laboratory of Inorganic Chemistry, Department of Chemistry and Applied Biosciences, Vladimir-Prelog-Weg 1-5/10, 8093, Zürich, Switzerland

3.1 Introduction

In the past years, polymer processing aiming at direct patterning and printing has witnessed an exponential growth, in particular in the rapidly growing field of flexible microelectronics, which demands fast and reliable patterning and printing technologies. The ability to develop miniaturized devices based on soft materials such as polymers combined or integrated with microfabricated substrates represents a key factor in one of the most important sectors of the microelectronics industry, with applications ranging from sensors to organic light-emitting diodes (OLEDs). However, there are still major issues concerning polymer patterning and printing and integration into devices due to their easy degradation or loss of their surface functionality, which is key to achieving the desired properties. In order to prevent this drawback, a variety of methods and approaches have been developed for polymer patterning and printing, from simple dispensing or soaking techniques to localized contact and noncontact patterning methods.

Spin coating has been used for several decades for the deposition of thin films. A typical process involves dispensing a small quantity of a fluid (a polymer dissolved in a proper solvent) onto the spinning substrate. Centripetal acceleration will cause most of the fluid to spread (also over the edge of the substrate), leaving a thin polymer film on the surface. The final film thickness and other properties will depend on the nature of the fluid (viscosity, drying rate, percent of the solid in the solution, surface tension, etc.) and the parameters chosen for the spinning process. Spin coating is a technique that offers a high degree of reproducibility [1]. However, it presents some disadvantages, that is, the lack of material efficiency. Typical spin coating processes utilize only 2–5% of the material dispensed onto the substrate [2], while the remaining 95–98% is propelled into the coating bowl and disposed of. Another disadvantage is the size of the substrates, that is, as the substrate size gets larger, the throughput of the spin coating process decreases. Large substrates cannot be spun at a sufficiently high rate in order to allow the film to thin and dry in a timely manner, which results in a decreased throughput.

Laser Printing of Functional Materials: 3D Microfabrication, Electronics and Biomedicine,
First Edition. Edited by Alberto Piqué and Pere Serra.

Another relatively easy process, spray coating, is the process of coating an object with a liquid spray of a polymer or any other fluid. Spray coating technology uses a spray produced by forcing a fluid under high pressure through a small nozzle (spray tip) making aerosols. The fluid emerges as a narrow sheet at a high speed. The friction between the fluid and the air disrupts the sheet, breaking it into fragments initially and ultimately into droplets. One of the advantages of this technique is that it allows a high production rate.

The main disadvantages of this technique are the limited control over the amount of fluid flow and that airless spray coating technologies are generally not considered to be capable of providing a very high finish quality [3]. In addition, another limitation of this process and also of the spin coating technique is that they do not offer lateral resolution and only complete layers can be obtained.

Inkjet printing is a noncontact patterning method, which provides a versatile and low-cost microfabrication capability. This noncontact digital technology can be used to pattern a variety of liquids including polymers, proteins, and various solvents onto different substrates, rigid or flexible, rough or smooth. The advantages of this technique are the high accuracy and resolution and that it does not require a master template [4]. However, among the most important limitations of inkjet printing, we enumerate clogging of the print heads and the reduced velocity.

Due to the fact that the aforementioned approaches do not meet all requirements, that is, precise positioning, repeatability, control of polymer layer thickness and roughness, novel techniques, which overcome these limitations, are developed. These techniques are mainly based on lasers.

Shortly after the discovery of lasers, researchers began irradiating every possible target material and phase. Three years after the discovery of laser, Breech and Cross [5] studied the laser vaporization and excitation of atoms from solid surfaces, while in 1965, Smith and Turner [6] deposited the first thin films using a ruby laser. Starting with that moment, laser ablation became more and more popular for the deposition of various materials as thin films.

Pulsed laser deposition (PLD) involves the interaction of a laser beam with a target material (solid or liquid) resulting in a plasma plume that transports the ablated species to a substrate, where a thin film is formed. PLD offers many advantages [7, 8]; however, it cannot be used for all types of polymers, biopolymers, and proteins, because the high laser fluences can result in photochemical or thermal decomposition. Even at relatively low fluences, some polymers are very photosensitive. To reduce the photochemical decomposition from the direct interaction of the UV laser light with organic and polymeric materials, a more gentle approach has to be used.

As an alternative to conventional deposition techniques, matrix-assisted pulsed laser evaporation (MAPLE) has proved to be an attractive method for the deposition of organic thin films [7, 9]. MAPLE is similar to PLD, but has a different target preparation procedure. In MAPLE, a material, for example, a polymer or a biomolecule, is dissolved in a solvent in concentrations of 0.1–5%, and the mixture is frozen, resulting in a solid target. Ideally, only the solvent will absorb the laser radiation. When the laser light irradiates the target, the solvent

is evaporated and the dissolved material (the organic material or the polymer) is collected on a substrate, in the same way as for PLD.

The laser methods described earlier are well suited for obtaining thin films of controlled thickness and roughness on different types of substrates. However, for precise patterning, that is, positioning soft materials onto different substrates with lateral resolution, different approaches must be considered.

One of these approaches (also based on an ablation process) is laser-induced forward transfer (LIFT, see Chapter 1 for a detailed description of this and other direct-write techniques). Briefly, in LIFT, the laser irradiates the material of interest (which is in thin-film form) through its transparent support, pushing the material toward the receiving substrate (placed parallelly and in close proximity). Only the material that is irradiated will be transferred, the laser spot defining the lateral shape of the deposition. The technique first appeared as a new deposition method for the direct writing of different dried inks to a glass substrate for the graphic industry [10–12]. At that point, it was called laser writing (LW) or material laser recording (MLR). However, the first report on LIFT was the "direct writing" of copper metal patterns onto fused-silica plates using a 193 nm ArF excimer laser [13, 14]. Based on this work, in the following years, several alternatives to LIFT were developed. These alternatives include reducing the transferred material pattern size [15] but also the transfer of complex materials, that is, soft, sensitive materials, which may be easily damaged by the laser pulses and result in the loss of functionality, for example, in the case of proteins.

Therefore, in order to reduce the risk of damaging the layer or the surface of the layer to be transferred and to improve the process efficiency, the donor substrate can be precoated with an intermediate layer, which is called dynamic release layer (DRL) [16] or sacrificial layer. To this day, many alternatives to the DRL–LIFT were developed, each with a different name; however, all are based on the same principle, that is, a locally confined laser energy to transfer the material of interest. The addition of an intermediate layer was initially used as a thermally activated DRL and then as a matrix in a process known as *matrix-assisted pulsed laser evaporation-direct write* (MAPLE-DW), a version of MAPLE for high-resolution patterning (see Chapters 1 and 2) [17]. In the MAPLE-DW technique, the material to transfer is embedded into a matrix, for example, a sacrificial polymer layer, usually a Matrigel or a gelatin layer. During MAPLE-DW, the matrix is evaporated due to the heat caused by the absorbed laser beam, which subsequently releases the material to transfer onto a receiving substrate.

Further on, researchers have used metallic layers (Ti, Au, Pt, Cr,) [18–22] as DRLs, which are especially useful for the transfer of biomolecules as they are biocompatible and easy to process. For example, in [23, 24], the authors use thin (50–100 nm) metal films to transfer different types of cells in a medium. They name the method absorbing film assisted-LIFT (AFA-LIFT) (see Chapter 4 for a detailed description). The principle of this process relies on using laser beams with a penetration depth smaller than the thickness of the sacrificial metallic layer. Upon laser irradiation, the metallic sacrificial layer thermally expands, and a volume of the suspension (in this case, the donor is a biological ink) is propelled to a receiver substrate [25]. Although successful for bio-applications, the main disadvantage of the metallic DRLs is related to contamination of the

transferred material as a result of the ablation process, that is, hot volatilized products. This can be detrimental in applications aiming at the fabrication of organic micro devices, as micro- and nanosized particles resulting from the laser ablation process may hinder the performance of the devices. In order to mitigate this effect, more recently, the use of thin and thick polymer layers as DRLs has been proposed. In [26, 27], the authors propose the use of thick (several micrometers) polyimide absorbing layers to transfer various materials in liquid phase (e.g., embryonic stem cells, 9-anthracenemethanol, and tris8-hydroxyquinolinealuminum Alq_3 organic luminophores). The authors name this process blister-actuated laser-induced forward transfer (BA-LIFT, see Chapter 5). The transfer mechanism in BA-LIFT relies on the absorption of the laser within a thin part of the polyimide DRL, near the donor–substrate interface, and the formation of a rapidly expanding blister of high-pressure decomposition products. Below a critical laser energy, the blister deforms plastically; however, it remains sealed, and the material to transfer continues to move toward the receiving substrate enabling a "clean" transfer, without contamination from the ablation products.

Another approach consists in the use of a photodecomposing polymer, that is, a triazene polymer (TP), which can minimize contamination and, in addition, can be applied to transfer both solid- and liquid-phase materials, unlike BA-LIFT, which is mostly used for transfer of liquid-phase materials. The TP in the laser molecular implantation (LMI) process [28] was eventually followed by the use of triazene as a propellant in the hollowing and transfer of polymethyl methacrylate [29]. This led to the use of the TP as a DRL in the printing of other sensitive materials (see Section 3.4).

This chapter reviews the LIFT process assisted by a UV degradable photopolymer as DRL (i.e., TP), from fundamentals to the application of the process for the transfer of a wide range of materials. In addition, a detailed analysis of the characteristics and process parameters of the TP-assisted LIFT process are reviewed, with emphasis on the possible applications of TP-LIFT in sensors or OLEDs.

3.2 Absorbing Release Layer – Triazene Polymer

Polymers that incorporate the triazene unit into the backbone were developed in the early 1990s, specifically for laser ablation [30]. The TPs contain aryl-triazene chromophores where a conjugated π system spreads over the three nitrogens and the benzene ring [31]. The chemical structure of the TPs is shown in Figure 3.1.

These polymers were initially studied for applications as resist for high-resolution microlithography [32]. However, regardless their large number of advantages, for example, formation of high-quality films, stability to storage, and one-step synthesis [26], these polymers are very sensitive to acids [33], which are used in industrial applications for the following lithography processing steps. Therefore, further alterations were considered in order to improve the quality of the ablation process and broaden their usage in applications such as micro-optics and laser-plasma thrusters for microsatellites [34].

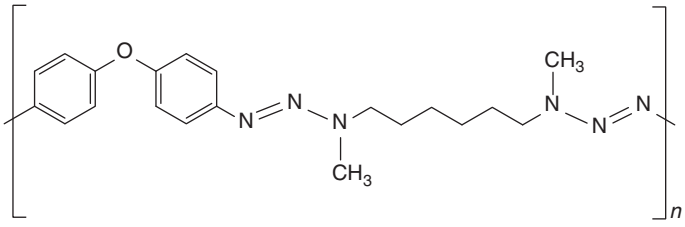

Figure 3.1 Chemical structure of the triazene polymer, which was used for most LIFT experiments.

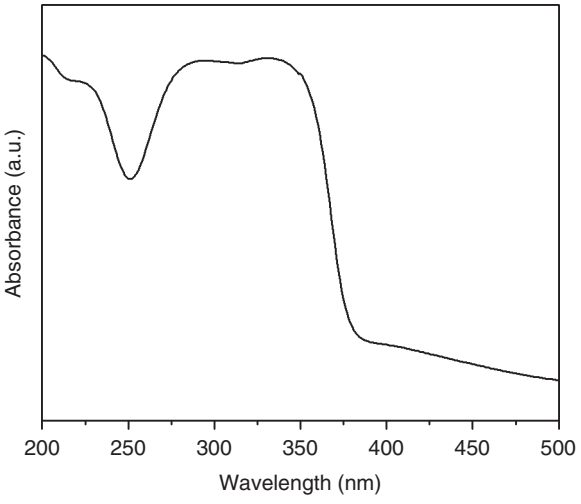

Figure 3.2 UV–vis absorption spectrum of a typical triazene polymer thin film, spin coated from chlorobenzene:cyclohexanone (1 : 1) solution.

A unique advantage of these polymers is the possibility to adjust the absorption maximum from 290 to 360 nm, making them appealing for irradiation with different wavelengths and different lasers. In the UV–vis absorption spectrum of a typical TP thin film (Figure 3.2), two distinct absorption maxima can be distinguished, one around 200 nm, which can be assigned to the aromatic system, and one around 330 nm, which corresponds to the triazene unit [35].

These two well-separated absorption regions led to numerous studies focused on the influence of different laser wavelengths on the ablation behavior. Higher ablation rates have been determined for irradiation wavelengths that excite the triazene system (266, 308, and 355 nm) compared to the ablation rates for shorter wavelengths (248 and 193 nm) [36]. In addition, a clear and well-defined ablation threshold fluence of 25 mJ/cm^2 ($\pm$5 mJ/cm^2) was observed for TP at an irradiation wavelength of 308 nm, while for irradiation with 248 nm, a much broader range of 16–28 mJ/cm^2 has been measured. For irradiation at 248 nm, carbonization of the polymer was detected upon irradiation, whereas the surface of the polymer remained unchanged after several laser pulses for irradiation with 308 nm [37].

In the following section, an overview of front- and backside ablation of the TP is presented. Although there is a multitude of laser wavelengths for which the ablation behavior has been studied, here we will only review TP ablation with the

XeCl laser operating at 308 nm. This is due to the fact that most of the studies in the literature focused on the transfer of functional materials (in solid and liquid phase) by LIFT were carried out with the XeCl laser, and the TP has the highest ablation rate and low threshold fluence at this wavelength (308 nm).

3.3 Front- and Backside Ablation of the Triazene Polymer

Front- and backside ablation behavior of the TP (Figure 3.3) has been studied in [38], by applying a time-resolved imaging technique (shadowgraphy) in order to gain information on the dynamic mechanism of the TP-assisted LIFT process. The experimental setup for such investigations consists in adding a camera with a microscopic objective perpendicular to the laser beam, that is, parallel to the sample surface, with the focus at the ablation spot. Illumination was obtained either by a probe laser pumping a fluorescent dye (rhodamine) or by a white-light nanosecond flash lamp placed on the camera axis on the opposite sample side. The delay between the pump and the probe laser pulses/flashlamp was set by a delay generator. Each picture was recorded with a different pulse and corresponds to a new position on the sample.

A sequence of photos taken for front-side ablation of a 500 nm thick TP layer for an irradiation fluence of 110 Jm/cm^2 is presented in Figure 3.4a. In comparison, a sequence of photos taken for backside ablation of a 460 nm thick TP film and for the same laser fluence (i.e., 110 mJ/cm^2) is shown in Figure 3.4b. In the case of front-side ablation, the film surface is on the right, while the laser pulse comes from the left, and in the case of backside ablation, the film surface is on the left, and the laser also comes from the left. In both figures, two propagating features can clearly be distinguished. The first feature is attributed to the shock wave caused by the pressure and temperature jump at the ablation spot, where a large amount of gas is released during the laser pulse. The second observable feature is different for the two cases of ablation: (i) in the case of front-side ablation, it is most probably formed by gaseous decomposition products from the polymer and (ii) in the case of backside ablation, the product front corresponds to an opaque object ejected from the substrate, that is, a flyer. In the case of front-side ablation, no particles are visible in the ablation plume, which confirms a clean and debris-free ablation of the triazene observed previously [39, 40]. In contrast, in the case of backside ablation, the presence of the flyer indicates that

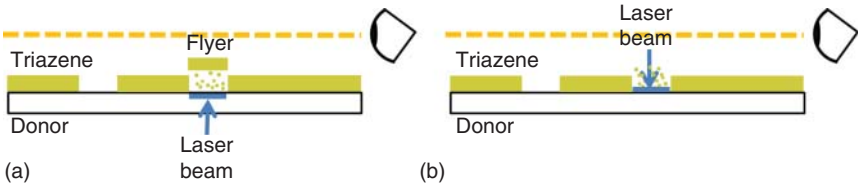

Figure 3.3 Schematic drawing of (a) backside ablation of a triazene polymer layer and (b) front-side ablation of a triazene polymer layer.

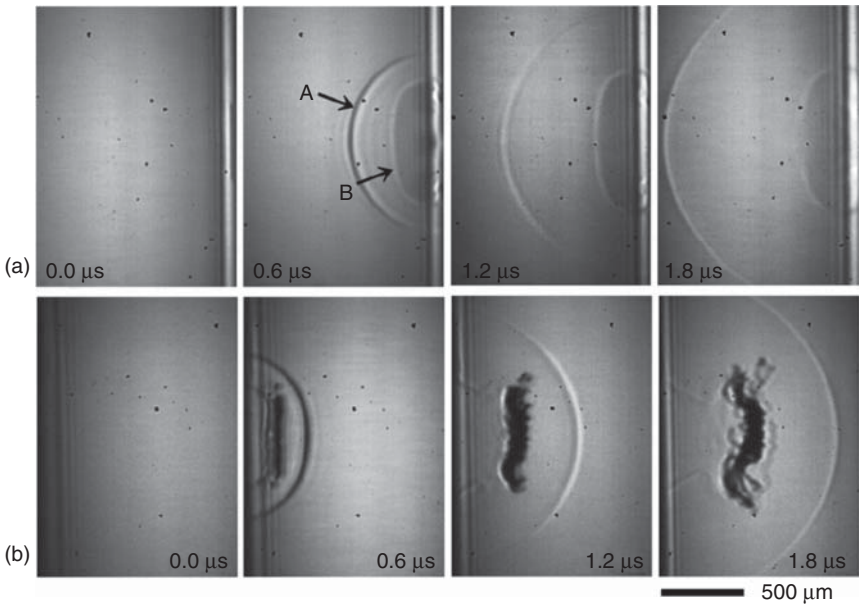

Figure 3.4 Sequence of photos taken for (a) front-side ablation of a 500 nm triazene polymer film at 110 mJ/cm^2 laser fluence; (b) backside ablation of a 460 nm triazene polymer film at 110 mJ/cm^2 laser fluence. (Fardel *et al*. 2009 [38]. Reproduced with permission of Elsevier.)

the entire triazene layer is not ablated by a single laser pulse at this fluence. The flyer consists of undecomposed polymer, which is ejected by the pressure thrust created during ablation and decomposition of the underlying part. In addition, the application of shadowgraphy for the study of the dynamics of TP-LIFT provided additional information, that is, on the flyer velocity, which when combined with the laser pulse length and the thermal effects gave insight into the energy generated by this process [41, 42]. Further work focused on a thermal analytical model has contributed to understanding the TP-LIFT process (at 308 nm) fundamentals [43]. The thermal model has been used to evaluate how fast the thermal energy is lost into the quartz substrates, and in the case of backside ablation, it is found that almost 50% is lost during the pulse length. In addition, in [44], the authors calculate the total energy transferred from the laser beam to the ablation species from the velocity of the shock wave. They found that a fraction of the laser energy was converted into mechanical energy (20–60%), while the remaining energy consumption occurred as thermal heat and mechanical loss into the substrate. In addition, the shock wave generated upon backside ablation was two times weaker than in the case of front-side ablation [44].

3.4 Examples of Materials Transferred by TP-LIFT

Aryltriazene polymers as sacrificial polymer release layers protect the transfer layer from the incident UV irradiation or generated heat, thus allowing highly

sensitive materials to be gently transferred and deposited. In addition, small and volatile organic fragments are formed by the laser-triggered photopolymer decomposition, and therefore, only a minimum of contamination of the transferred deposits may be expected. This is a substantial advantage compared to metal absorbing layers, which are known to be codeposited with the transferred material after laser-induced volatilization during the LIFT process [45, 46].

The use of aryltriazene photopolymers as sacrificial layers in LIFT applications was demonstrated with various highly sensitive materials in solid phase, including metals (i.e., Al) and oxides (such as $Ca_3Co_4O_9$), but also "soft" materials (some in liquid phase), that is, liposomes or cells. A list of the most representative materials is compiled in Table 3.1.

In [29], the first transfer of a polymethyl methacrylate polymer layer (as thin solid films) is reported, which opened up new possibilities for sensor fabrication where chemically selective polymers should be precisely deposited onto microsensor structures. In addition to the resolution requirement, the deposited polymer patterns should maintain their surface intact, that is, not alter their surface chemistry. Homogeneous, well-defined, and hole-free polyethyleneimine (PEI), polyepichlorohydrin (PECH), and polyisobutylene (PIB) pixels with low surface roughness were deposited from donors with triazene photopolymer

Table 3.1 Materials deposited through TP-LIFT.

Material	Laser and pulse length	Substrate	References
Mammalian cells	ArF (193 nm), ns	Glass	[47]
Quantum dots	ArF (193 nm), ns	Glass wafers coated with ITO	[48]
Liposomes	ArF (193 nm), ns	Glass	[49]
$Gd_3Ga_5O_{12}$	Ti:sapphire (800 nm), fs	Si wafer	[50]
Al	XeCl (308 nm), ns	Glass	[39, 51]
Polyisobutylene, polyethylenimine, polyepichlorohydrin	XeCl (308 nm), ns Nd:YAG (355 nm), ns	Glass, Al interdigitated transducers	[52–56]
Ag paste	Nd:YAG (355 nm), ps	Glass	[57]
Polystyrene microbeads	XeCl (308 nm), ns	Thermanox coverslips	[58, 59]
Single-walled carbon nanotubes	XeCl (308 nm), ns	Pt interdigitated transducers	[60]
Semiconducting oligomer	KrF (248 nm), ns Nd:YAG (355 nm), ps	Si/SiO_2	[61]
$Ca_3Co_4O_9$	XeCl (308 nm), ns	PDMS	[62]
Gelatine dyed with eosin	XeCl (308 nm), ns	Glass	[39]
OLED (Al/MEH-PPV)	XeCl (308 nm), ns	ITO-covered glass	[63, 64]
Polymer light-emitting diodes (Al/PFN)	XeCl (308 nm), ns	Glass/ITO/PEDOT:PSS/PVK	[65]
Methylcellulose	XeCl (308 nm), ns	Glass	[39]
$SnCl_2(acac)_2 \rightarrow SnO_2$	XeCl (308 nm), ns	Pt electrodes	[66, 67]

layers with thicknesses in the range of 60–300 nm after process optimization [52, 53]. LIFT of PEI, PIB, and PECH pixels onto surface acoustic-wave (SAW) structures allowed measurement of different chemical analytes [54, 55].

In addition, with TP-LIFT, it was possible to fabricate microarrays of polystyrene microbeads (PS-μbeads) on Thermanox coverslip surfaces without any specific immobilization process. For this, a XeCl excimer laser (with a top hat beam profile) was shaped using a $2 \times 2\,mm^2$ rectangular aperture and demagnified four times to ablate square PS-pixels of $500 \times 500\,\mu m^2$. TP layers of 100 nm were used as DRL to propel close-packed monolayers of PS-μbeads, very adherent to the Thermanox substrates and which do not suffer any chemical decomposition during transfer [58, 59]. A sequence of pictures taken for backside ablation of a PS-microbeads pixel on top of a 100 nm thick TP layer together with the corresponding SEM images of the pixel and its surface morphology are shown in Figure 3.5. The fact that these arrays can be produced cost-effective and time-effective with a minimum sample volume required suggests that TP-LIFT is a promising technique for transferring PS-bead pixels, which can therefore be applied in biochip applications.

The use of the TP as DRL also enables the accurate LIFT deposition of metal films. Aluminum film pixels ($500\,\mu m \times 500\,\mu m$, 80 nm thin) transferred from a quartz substrate coated with a 350 nm thick triazene layer showed clear-cut edges and a homogeneous layer morphology without traces of splashing or debris outside the pixel area for laser fluences in the range of 490–570 mJ/cm^2 [39]. It has been found that the mechanical as well as the thermophysical material properties of the transfer layer and carrier substrate have significant effects on the transfer results. In addition, the transfer dynamics of Al layers has been investigated by nanosecond time-resolved imaging techniques [51, 68]. The shadowgraphy data show that the Al flyer is completely destroyed by the shock wave when high laser fluences are applied, while in the case of low laser fluences (after 2 μs), only slight bending at the edges of the flyer may be observed [51, 68].

In [47], the transfer of viable neuroblast cells using a 193 nm ArF laser was reported. LIFT was carried out with 90, 110, and 140 nm thick sacrificial TP as DRL, and ribbons of B35 neuroblast cells were transferred from a donor to a receiver substrate over a gap of 150 μm above the threshold fluence for cell transfer of 50 mJ/cm^2. The biocompatibility of the TP was assessed with different cell lines, for example, osteoblasts, myoblasts, and endothelial cells, and the results indicated very good adhesion. In addition, 48 h post transfer, the cells showed intact preservation of nuclei with well-developed axonal extensions, demonstrating that the technique is applicable in creating patterns of viable cells at low fluences.

Further on, in [49], the authors report the transfer of a biomembrane model system, that is, liposomes in solution (liquid-phase TP-LIFT) in regular patterns onto glass substrates (detailed information is presented in Chapter 14). After a careful optimization of the laser transfer parameters, for example, influence of target–substrate distance, thickness of the applied TP layer, and laser fluence on the pattern sizes and shape, clearly circular, well-defined patterns can be obtained for relatively low laser fluences in the range of 40–60 mJ/cm^2. The fact that these biomembrane patterns can be obtained in a time-effective manner

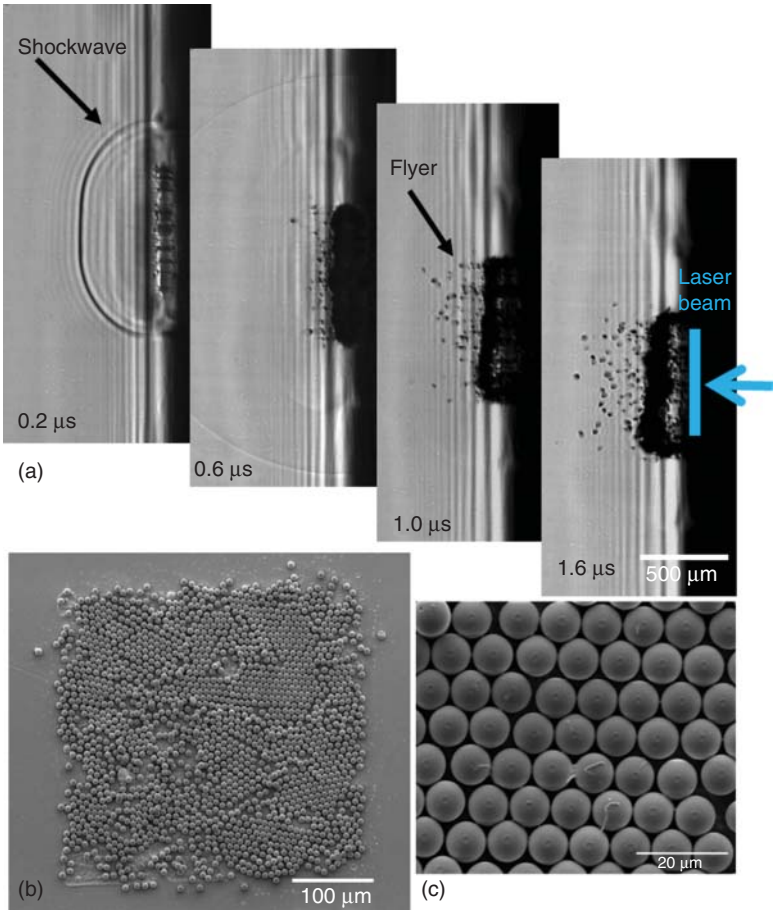

Figure 3.5 (a) Sequence of pictures taken for backside ablation of a PS-microbead pixel on top of a 100 nm thick triazene polymer layer at 1.5 J/cm^2 laser fluence. (b) SEM image of a PS-microbead pixel transferred at 2.25 J/cm^2 laser fluence. (c) SEM image of the surface morphology of the PS-microbeads transferred at 1.5 J/cm^2 laser fluence. (Palla-Papavlu *et al*. 2010 [58]. Reproduced with permission of AIP.)

and with a minimum sample volume suggests that they can be ultimately applied in biosensors or drug delivery systems.

Another interesting application of TP-LIFT is the successful transfer of semiconducting multispectral nanocrystal quantum dots (NCQDs) into laterally patterned arrays [48]. A 40 nm thick TP layer was used for the transfer of CdSe nanoquantum dots (5 and 6 nm in diameter) onto ITO-coated substrates. A 6 × 6 red and yellow array with pixel sizes of 800 µm was demonstrated. Photoluminescence of the NCQDs before and after transfer was found to be nearly unchanged, indicating the conservation of material functionality during the transfer.

Finally, to prove the validity of the photopolymer-based LIFT approach, working miniaturized model OLED devices have been fabricated for the first time

using LIFT [63]. Detailed information of the fabrication of OLEDs by TP-LIFT is given in Section 3.5.1 and also in Chapter 12.

3.5 First Demonstration of Devices: OLEDs and Sensors

In the previous sections of this chapter, some of the advantages and limitations preventing the adoption of TP-LIFT in printing different materials have been presented. Although TP-LIFT has been extensively used to transfer a wide range of materials, for material integration into functional devices, a trade-off between the various experimental parameters and limitations of the technique must be taken into account. If for the fabrication of OLEDs, complete functional layers must be transferred, the transfer can take place with the metal electrode sandwiched between the TP-DRL and the electroluminescent polymer, thus additionally protecting the electroluminescent polymer; in the case of polymers for sensor applications, the process is even more "delicate." When transferring polymers for sensing applications, the surface of the polymer that is in contact with the TP as DRL is actually the sensing surface, and no damage, contamination, or functionalization of the surface should take place during or post transfer. Here, we will only briefly present the main results of TP-LIFT for the fabrication of functional OLEDs and sensors (for both examples, the transfer is carried out from solid donor layers). Please refer to Chapters 12 and 13 for detailed description of LIFT for microdevice fabrication (Chapter 12), that is, OLEDs, thin-film transistors, and sensors and biosensors (Chapter 13).

3.5.1 Organic Light Emitting Diode (OLEDs)

The first work on the transfer of OLED devices was undertaken in 2007 [63]. This was one of the biggest breakthroughs in the field of LIFT, not just for OLEDs. Good functionality and pixel morphology were observed, as shown in Figure 3.6.

The devices reported in [63] were realized in the simplest architecture, that is, an electroluminescent material sandwiched between an anode and a cathode. The anode was a transparent tin-doped indium oxide (ITO), which was used as receiving substrate onto which an aluminum/MEH-PPV (poly[2-methoxy-5-(2-ethylhexyloxy)-1,4-phenylenevinylene]) bilayer was LIFTed. The bilayer, that is, the cathode and the electroluminescent materials Al/MEH-PPV with thickness of 80 nm Al and 90 nm MEH-PPV were deposited onto a 100 nm thick TP layer. The laser fluence applied for the successful transfer was of 250 mJ/cm^2 (308 nm XeCl laser). Bilayer transfers were carried out with the donor and receiver substrates in as close contact as possible. Small cracks in the devices were a minor problem, but a larger problem was the reproducibility. On a single sample, about eight pixels could be deposited on the two ITO edges. Even at the same fluence, huge variations in pixel morphology could be observed on a single substrate, and from sample to sample, the variation was even larger. However, the characterization of the transferred pixels by luminance and emission spectroscopy revealed the same characteristics as those of a similar device made by well-established techniques.

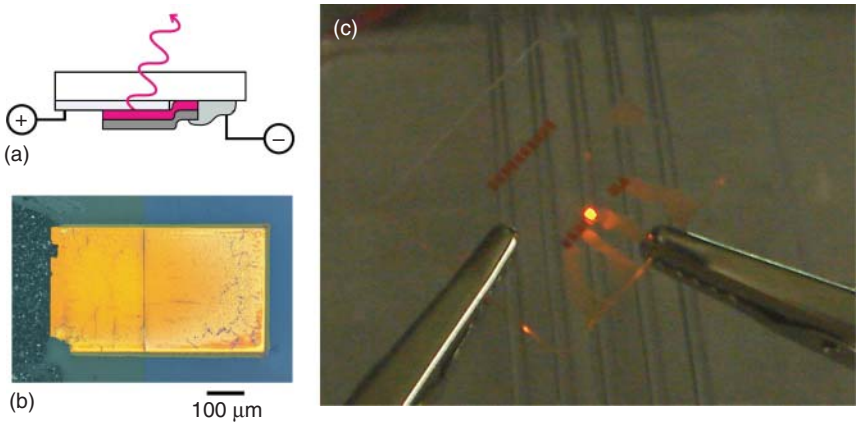

Figure 3.6 (a) Scheme of the device architecture with two electrodes (ITO anode and Al cathode) and the MEH-PPV light-emitting layer. (b) Al/MEH-PPV transferred onto the ITO substrate. (c) Image of the successful operation of one of the transferred devices. (Fardel *et al*. 2007 [63]. Reproduced with permission of AIP.)

The fact that sensitive materials such as MEH-PPV could be transferred without altering the functional properties proves that the LIFT technique with a TP as sacrificial layer is very well suited to the transfer of sensitive materials.

Later works [64, 65] have shown that by optimizing the laser transfer process, optimized devices could be fabricated.

In [64], the functionality of the OLEDs has been improved by modifying charge injection in the devices. This has been realized by adjusting both the cathode and anode by adding additional layers, that is, electron-injecting and hole-transporting layers. The scheme of the TP-LIFT for the fabrication of OLED pixels/devices is shown in Figure 3.7a. In addition, in [64], it has been shown that by adding a thin film of poly(3,4-ethylenedioxythiophene) polystyrene sulfonate (PEDOT:PSS) onto the ITO receiver substrate, it was possible to achieve a "softer" transfer, that is, to reduce the laser fluence required for the transfer, that is, from 250 to 80 mJ/cm^2. The authors suggest that this effect is due to the stronger attractive force interactions between the flyer and the PEDOT:PSS layer. The transferred pixels exhibited far superior and more reliable device characteristics compared to the devices LIFTed onto plain ITO. Finally, the LIFTed pixels were compared with the conventionally fabricated devices. The overall performance of the LIFTed poly(ethylene)oxide (PEO)-containing pixels was slightly lower than for conventional devices, possibly because of oxygen and water damage by combining the substrates together in air, but the plain MEH-PPV device showed elevated performance, presumably mainly due to the different light-emitting polymers (LEP)/Al interface [69]. An example of two working devices fabricated by LIFT that showed the distinctive orange-red electroluminescence is presented in Figure 3.7b.

In addition, further optimization and refinement of the LIFT process itself, that is, controlling the gap between the donor and the receiver, the usage of the TP layers thicker than 150 nm, together with carrying out all laser transfer in

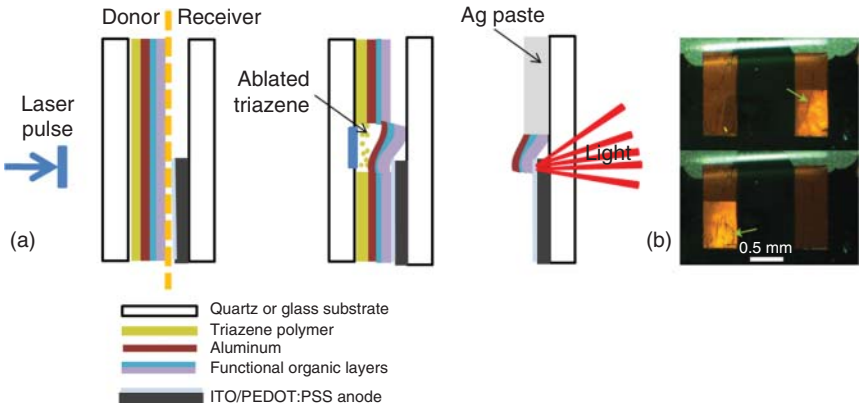

Figure 3.7 (a) Scheme of the TP-LIFT for fabricating an OLED pixel/device. (b) Electroluminescence from two LIFTed devices with the architecture ITO/PEDOT:PSS/MEH-PPV:PEO/Al. The light-emitting section of the diodes is the lower half, where the aluminum cathode overlaps with the ITO anode. (Shaw-Stewart *et al*. 2011 [64]. Reproduced with permission of ACS Publications.)

a controlled atmosphere (vacuum), led to the successful fabrication of three-color OLEDs (see Chapter 14).

Further works have focused on varying the processing parameters together with the characteristics of LIFT for improving the OLED device performances. One of the main issues related to LIFT assisted by a TP layer is of solvent orthogonality of the different polymers in adjacent layers. In order to solve this issue, a strict orthogonality in the solubility of different materials or subsequent selective cross-linking of previously solution-deposited layers is required. Therefore, for the fabrication of OLEDs by sequential LIFT, poly[(9,9-bis(3′-(*N*,*N*-dimethylamino)propyl)-2,7-fluorene)-alt-2,7-(9,9-diocty-fluorene)] (PFN) was chosen, which could be dissolved in methanol:DMF (dimethylformamide) (99 : 1) solution and directly spin coated on top of the TP layer (insoluble in that solution). However, the sequential LIFT of PFN and Al single layers to fabricate a functioning PFN PLED was very positive, but the device characteristics were much poorer than the PFN conventional device and the normal bilayer LIFTed PFN pixel, with a much higher operating voltage and poorer efficiency. A positive fact was that the electroluminescence spectrum was completely unchanged, suggesting that the chemical structure was unaltered. In addition, the adsorption of a layer of *tert*-butyl acrylate (TBA) onto the aluminum cathodes led to a significant improvement in device performances. The TBA layer was used with the purpose of promoting electron injection from the aluminum cathode, thus increasing the device efficiency [64].

3.5.2 Sensors

Another breakthrough in the field of TP-LIFT is the successful demonstration of chemical sensors for the detection of volatile organic compounds (VOCs) and warfare agents. For detailed information on sensor fabrication by LIFT,

please refer to Chapter 13. Several polymers have been checked from the point of view of their properties in the form of thin films: PIB, PEI, and polyepichlorohydrin (PECH). PEI with the molecular formula $(C_6H_{21}N_5)_n$, PECH $[CH(CH_2Cl)CH_2O]_n$, and PIB $[CH_2(CH_3)_2]_n$ are used for the detection of the nerve agent sarin (GB), simulants such as dimethyl methyl phosphonate (DMMP), and also hydrocarbons (acetone) and esters (i.e., ethyl acetate). The ability of the polymers to form weak hydrogen bonds with the target analyte molecules is the most basic functionality prescribing the polymers' utility in the design of a useful chemical warfare agent detector.

The most common and studied type of chemical detectors are the SAW sensors due to their remarkable performances in terms of high sensitivity, portability, low cost, and easy deployment [70, 71, 80]. These devices are based on a SAW resonator, solidly mounted resonator (SMR), or a delay line, where the propagation path is coated with a chemically interactive membrane, that is, a polymer designed to detect a specific analyte. The main issue related to the development of performant SAW resonators for the detection of toxic and chemical species is the poor reliability caused by the lack of accuracy in placing the polymer membranes onto the SAW devices. The sensitivity of the SAW resonators is dependent on the amount of vapor adsorbed by the surface of the polymer overlayer and also by the SAW's inherent ability to respond to the physical changes in the overlaying film. Therefore, it is very important to precisely place the polymer coating and moreover for the coating to have the correct thickness and roughness and desired functionality on the surface.

PIB, PEI, and PECH were deposited by laser-based methods as chemical interactive membranes onto the SAW sensor structures. Preliminary work on the DRL-LIFT of different chemoselective polymers, that is, PEI, PIB, and PECH, has shown that a careful optimization of different transfer parameters, that is, the laser fluence, donor film morphology, single- and multiple-pixel deposition, is critical for the successful microfabrication of the chemical sensors based on SAW devices [52, 53]. Additional studies have shown that a separation distance between the donor and the receiver substrates results in damage of the transferred material [69]. All transfer experiments were therefore carried out in close contact between the donor and the receiver. The studies reported in [52, 53] have shown that in order to minimize scattering and diffraction of the SAW devices, it is important to (i) improve the polymer pixel morphology by using TP as a DRL compared to the LIFT process without a DRL; (ii) use the 308 nm wavelength (it yields better results, i.e., clean-cut pixels) instead of 266 nm irradiation; (iii) use polymer films with thicknesses below 60 nm. Optical microscopy images of PIB, PECH, and PEI polymers transferred by LIFT onto different types of SAW devices are shown in Figure 3.8a,b.

In addition to sensor fabrication by TP-LIFT, a sealed chamber containing electronic oscillators, one for each sensor, was designed and fabricated. In order to obtain an optimized and complete measuring system, resonators without any coating were provided as reference. The TP-LIFT-coated SAW and SMR sensors were tested to evaluate the performances with respect to sensitivity, resolution, and response time. The first measurements were carried out onto single SAW and SMR sensors by using the Network Analyzer in order to track the frequency

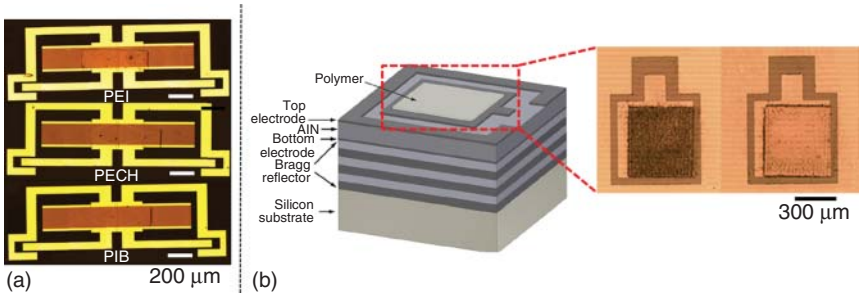

Figure 3.8 (a) Optical microscopy images of PIB (bottom), PECH (middle), and PEI (top) polymers transferred by LIFT onto two-port SAW devices. Dinca *et al*. 2013 [72]. Reproduced with permission from Romanian Reports in Physics.) (b) Schematic drawing of the SMR (left side) and optical microscopy images of SMR devices coated with PEI polymer deposited at 400 mJ/cm^2 (left) and 300 mJ/cm^2 (right) laser fluence. (Cannata *et al*. 2012 [55]. Reproduced with permission of Elsevier.)

shifts of the resonance peak due to various concentrations of different analytes. The devices under test were placed in a sealed chamber where the total gas flow was kept constant and the analyte concentrations were in the range of parts per million. The responses of the PEI, PIB, and PECH coated devices to different concentrations of DMMP, GB, ethyl acetate, and acetone were evaluated. The tests carried out with the SAW resonators [54] showed good performances of the SAW sensor fabricated by TP-LIFT, in particular for DMMP and GB. The obtained sensitivities for DMMP are similar to the results reported in the literature where the same polymers were used, however, deposited on the surface of the sensors with more mature and well-established techniques (airbrush, spray coating, screen printing) [73, 74], proving thus that the TP-LIFT process does not strongly alter the surface chemistry of the polymers. In addition, a remarkable result is the sensitivity obtained for sarin (~650 Hz/ppm) that is one order of magnitude higher than those obtained using DMMP (~66 Hz/ppm). The lowest concentration of measured GB was lower than the median lethal dose (18 ppm). The time responses of the three sensors for two concentrations of ethyl acetate (EtOAc) together with the response curve for PECH, PEI, and PIB sensors upon exposure to different concentrations of DMMP are shown in Figure 3.9a,b.

Furthermore, when exposing the SMR devices to different concentrations of DMMP [54], that is, between 22 and 127 ppm, fast and reversible responses are obtained, with the highest sensitivity obtained for PEI and followed by PIB and PECH. The frequency response of an SMR before and after deposition of 13 nm thick PECH film and the response curves of coated SMR sensors (PEI, PIB, and PECH polymers) for DMMP are presented in Figure 3.9c,d.

The SMR has several advantages, that is, the simple and well-known planar fabrication technologies and the small size of resonator. Moreover, the use of Bragg reflector ensures a robust design allowing simple and straightforward polymer depositions by LIFT. Finally, considering the flexibility and the micron-scale lateral resolution obtainable by LIFT and the possibility to integrate a large number

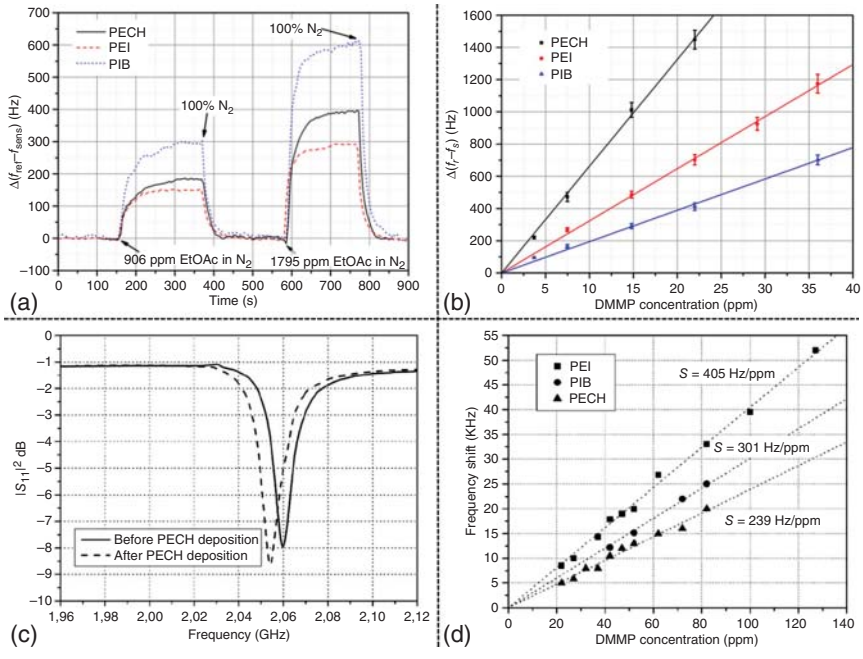

Figure 3.9 (a) Time response of the three SAW sensors for two concentrations of EtOAc. (b) Response curve for PECH, PEI, and PIB sensors upon exposure to different concentrations of DMMP. (Di Pietrantonio *et al*. 2012 [54]. Reproduced with permission of Elsevier.) (c) Frequency response of an SMR before and after deposition of 13 nm thick PECH film. (d) Response curves of coated SMR sensors (PEI, PIB, and PECH polymers) for DMMP. (Cannata *et al*. 2012 [55]. Reproduced with permission of Elsevier.)

of SMRs on a single silicon chip, the proposed solution is an excellent candidate for implementation of sensor arrays using different sensitive polymers.

3.6 Variation of the DRL Approach: Reactive LIFT

In recent years, sensor development and improvement received great attention from industry and research. A direct-writing technique such as LIFT is a promising method for commercial sensor coating. It is solvent free, and a large variety of materials can be transferred with high lateral resolution onto nearly every substrate. It would be a promising alternative to replace, for example, photolithographic steps or inkjet printing. One other advantage is that large-area donor substrate can be prepared by different well-established methods such as spin coating, sputtering, evaporation, or drop casting [75, 76].

A new approach, that is, reactive LIFT (rLIFT), has been evaluated as an alternative method to LIFT, which allows the integration of metal-oxide semiconductor materials, that is, SnO_2 for their use in microsensors. In rLIFT, the donors are UV-absorbing metal complex precursors (i.e., metal acetylacetonates), which upon absorption of the laser light partially decompose to SnO_2 [77], thus making the transfer layer a DRL. Solution-based precursors are in particular appealing

due to their low deposition (growing) temperatures, which make them suitable for flexible substrates, and good potential for scaling-up. During the past decade, a large number of metal oxides have been prepared from metal acetylacetonates, for example, TiO_2, In_2O_3, SnO_2 [78] and more recently ZnO nanowires [79]. rLIFT is a unique technique that combines the advantages of the low decomposition temperatures of the acetylacetonates together with the spatial resolution of the laser-based method. The transformation of the metal precursor to SnO_2 takes place partially during laser transfer as a result of the photochemical and thermal processes, which in this particular case are an advantage as they shorten the fabrication process. Therefore, rLIFT has proven great potential for the integration of active materials into micro-sensing devices.

In recent works [67], the rLIFT technique was demonstrated for the fabrication of SnO_{2-} and Pd:SnO_2-based gas sensors. The donors were UV-absorbing metal acetylacetonates spin coated onto fused-silica substrates. The UV–vis absorption spectrum of a typical $SnCl_2(acac)_2$ thin film with a thickness of 900 nm used as a donor in the rLIFT experiment together with the chemical structure of the $SnCl_2(acac)_2$ is shown in Figure 3.10. Previous studies have shown that by a careful choice of the transfer parameters, regular, well-defined SnO_2 pixels could be printed onto glass substrates from donor films of metal complex precursors. The laser fluence was an important parameter to achieve a regular, debris-free transfer and therefore was investigated thoroughly. The range of laser fluences for which successful transfers were obtained, that is, SnO_2 pixels with a surface structure comparable to the donor film, was 200–400 mJ/cm^2. The transferred pixels were in the range of 900 nm–1 μm thickness, as determined by measuring their height with a profilometer.

In [67], the authors have shown that rLIFT was an appropriate technique for fabricating efficient SnO_{2-} and Pd:SnO_2-based sensors. An example of a SnO_2 sensor printed by rLIFT is shown in Figure 3.11a. Measuring the base resistance of the rLIFTed sensors in dry and humid air, it was concluded that the SnO_2 transferred pixels have a resistance in a suitable range for sensing applications.

Further on, analyzing the sensor responses toward C_2H_5OH revealed that the laser-transferred SnO_2 pixels had a very high response, and most of the

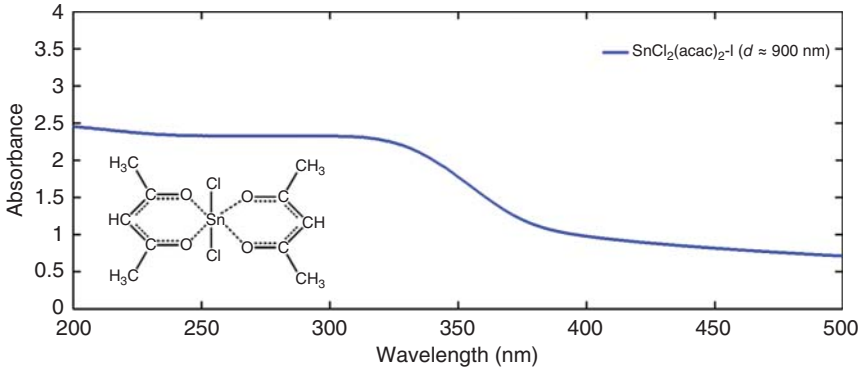

Figure 3.10 UV–vis absorption spectrum of a typical $SnCl_2(acac)_2$ thin film with a thickness of 900 nm. Inset: Chemical structure of $SnCl_2(acac)_2$.

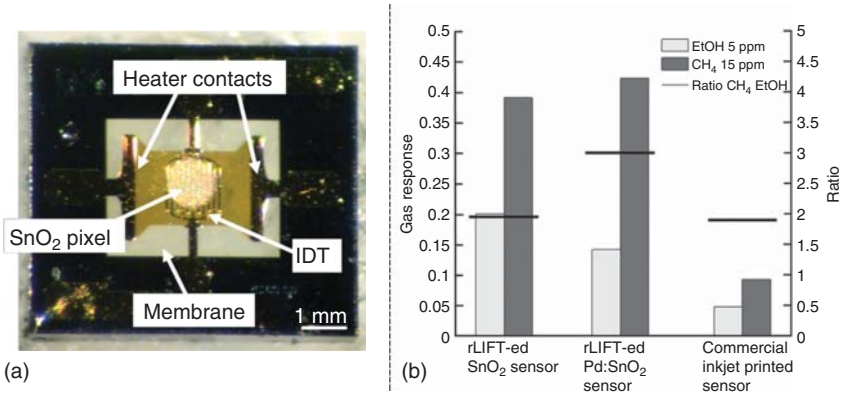

Figure 3.11 (a) SnO_2 rLIFTed pixel onto a commercial Microsens semiconductor gas sensor (MSGS) structure. (b) Sensor responses to 5 ppm of ethanol (at 350 °C) and 15 ppm of methane (at 500 °C). (Palla-Papavlu *et al*. 2016 [67]. https://www.ncbi.nlm.nih.gov/pmc/articles/PMC4846859/. Used under CC BY 4.0.)

sensor-like pads were close to saturation even when exposed to 10 ppm of C_2H_5OH. The rLIFTed sensor-like pads were stable over approximately 1 year.

Another key analyte for SnO_2 gas sensors was the detection of CH_4. With the rLIFTed SnO_2 pixels, 50 ppm CH_4 could be detected in dry air. Moreover, a comparison between the SnO_2 sensors fabricated by rLIFT and sensors fabricated by drop casting the metal complex precursor onto the sensor-like pads was carried out. The sensor responses were much lower in comparison with the rLIFTed sensors. Therefore, it can be assumed that the rLIFT process was the key factor to achieve SnO_2 pixels with high gas responses. The high response toward C_2H_5OH and CH_4 determined on the sensor-like pads was successfully confirmed. The sensor response of the SnO_2 rLIFTed sensors had four times better performance than the commercial inkjet printed sensors using the SnO_2 and the same sensing structure. In addition, the Pd-doped SnO_2 rLIFTed showed four times better response toward CH_4 than the commercial inkjet printed sensor. The sensor responses to 5 ppm of ethanol and 15 ppm of methane are shown in Figure 3.11b. The black line in Figure 3.11b indicates the ratio ($S[CH_4]/S[C_2H_5OH]$) between the two sensitivities to visualize the influence of Pd doping. This suggested that rLIFT could be a competitive alternative to commercial printing techniques, that is, sputtering or inkjet printing for fabricating high-performance sensors.

3.7 Conclusions and Perspectives

Applications in the field of microelectronics require processing techniques that allow material patterning and printing with high spatial resolution and reproducibility. LIFT has been classified as an emerging additive printing technique, competing with more mature techniques, such as inkjet or screen printing. From the first reports on this technique 30 years ago to the present day, several modifications to LIFT were developed, which try to accommodate different material

phases, that is, from liquid to solid, and also their integration into functional devices. These modifications include, for example, the addition of a DRL, which would facilitate (and protect) the intact transfer of materials.

In this chapter, we focus on the LIFT process assisted by a TP as a DRL and show some of the advantages and limitations preventing the adoption of this technique in patterning and printing of solid- and liquid-phase materials and devices (sensors and OLEDs). TP-LIFT, as an additive manufacturing process, offers advantages that make it an ideal technique in applications aiming at non-traditional manufacturing, where high resolution and high printing speed would open up the possibilities for competitive patterning and printing of materials.

In this context, the potential for additive printing is to be more economical and more environmentally friendly than the current methods. However, patterning and printing by TP-LIFT and LIFT in general still present challenges, and new ways to deliver both structural and functional materials in liquid or solid form need to be addressed.

Acknowledgments

Financial support from the Paul Scherrer Institute, the Commission for Technology and Innovation CTI (project no. 16713.1 PFNM-NM) and the European Commission – Seventh Framework Program (FP7-ICT project no. 247868, eLIFT) is gratefully acknowledged.

Conflict of Interest

The authors declare no competing interests.

References

1 Caliendo, C., Fratoddi, I., Russo, M.V., and Sterzo, C.L. (2003) Response of a Pt-polyyne membrane in surface acoustic wave sensors: experimental and theoretical approach. *J. Appl. Phys.*, **93** (12), 10071–10077.
2 Haaland, P., McKibben, J., and Paradi, M. (1995) Fundamental constraints on thin film coatings for flat-panel display manufacturing. 2nd Display Manufacturing Technology Conference, pp. 79–81.
3 Bruening, M. and Dotzauer, D. (2009) Polymer films: just spray it. *Nat. Mater.*, **8**, 449–450.
4 de Gans, B.J., Duineveld, P.C., and Schubert, U.S. (2004) Inkjet printing of polymers: state of the art and future developments. *Adv. Mater.*, **16** (3), 203–213.
5 Breech, F. and Cross, L. (1962) Optical microemission stimulated by a ruby MASER. *Appl. Spectrosc.*, **16**, 59.
6 Smith, H.M. and Turner, A.F. (1965) Vacuum deposited thin films using a ruby laser. *Appl. Opt.*, **4**, 147–148.

7 Chrisey, D.B., Piqué, A., McGill, R.A., Horwitz, J.S., Ringeisen, B.R., Bubb, D.M., and Wu, P.K. (2003) Laser deposition of polymer and biomaterial films. *Chem. Rev.*, **103** (2), 553–576.

8 Brodoceanu, D., Scarisoreanu, N.D., Filipescu, (.M.).M., Epurescu, G.N., Matei, D.G., Verardi, P., Craciun, F., and Dinescu, M. (2004) Pulsed Laser deposition of oxide thin films, in *Plasma Production by Laser Ablation* (eds S. Gammino, A.M. Mezzasalma, F. Neri, and L. Torrisi), World Scientific, pp. 41–46.

9 Schou, J. (2009) Physical aspects of the pulsed laser deposition technique: the stoichiometric transfer of material from target to film. *Appl. Surf. Sci.*, **255**, 5191–5198.

10 Braudy, R.S. (1969) Laser writing. *Proc. IEEE*, **57**, 1771–1772.

11 Brisbane, A.D. (1971) Pattern deposit by laser. U.S. Patent 3,560,258, filled and issued May 31, 1967 issued Feb 2, 1971.

12 Levene, M.L., Scott, R.D., and Siryj, B.W. (1970) Material transfer recording. *Appl. Opt.*, **9** (10), 2260–2265.

13 Bohandy, J., Kim, B.F., and Adrian, F.J. (1986) Metal deposition from a supported metal film using an excimer laser. *J. Appl. Phys.*, **60** (4), 1538–1539.

14 Bohandy, J., Kim, B.F., Adrian, F.J., and Jette, A.N. (1988) Metal deposition at 532 nm using a laser transfer technique. *J. Appl. Phys.*, **63** (4), 1158–1162.

15 Sametoglu, V., Sauer, V.T.K., and Tsui, Y.Y. (2013) Production of 70-nm cr dots by laser-induced forward transfer. *Opt. Express*, **21** (15), 18525–18531.

16 Tolbert, W.A., Lee, I.-Y.S., Doxtader, M.M., Ellis, E.W., and Dlott, D.D. (1993) High-speed color imaging by laser ablation transfer with a dynamic release layer: fundamental mechanisms. *J. Imaging Sci. Technol.*, **37** (4), 411–421.

17 Piqué, A., Chrisey, D.B., Auyeung, R.C.Y., Fitz-Gerald, J., Wu, H.D., McGill, R.A., Lakeou, S., Wu, P.K., Nguyen, V., and Duignan, M. (1999) A novel laser transfer process for direct writing of electronic and sensor materials. *Appl. Phys. A*, **69** (7), S279–S284.

18 Dinca, V., Fardel, R., Di Pietrantonio, F., Cannatà, D., Benetti, M., Verona, E., Palla-Papavlu, A., Dinescu, M., and Lippert, T. (2010) Laser induced forward transfer: an approach to single-step polymer microsensor fabrication. *Sens. Lett.*, **8** (3), 436–440.

19 Boutopoulos, C., Tsouti, V., Goustouridis, D., Chatzandroulis, S., and Zergiotti, I. (2008) Liquid phase direct laser printing of polymers for chemical sensing applications. *Appl. Phys. Lett.*, **93**, 191109.

20 Fitz-Gerald, J.M., Pique, A., Chrisey, D.B., Rack, P.D., Zeleznik, M., Auyeung, R.C.Y., and Lakeou, S. (2000) Laser direct writing of phosphor screens for high-definition displays. *Appl. Phys. Lett.*, **76** (11), 1386–1388.

21 Fernande-Pradas, J.M., Colina, M., Serra, P., Dominguez, J., and Morenza, J.L. (2004) laser-induced forward transfer of biomolecules. *Thin Solid Films*, **453–454**, 27–30.

22 Barron, J.A., Wu, P., Ladouceur, H.D., and Ringeisen, B.R. (2004) Biological laser printing: a novel technique for creating heterogeneous 3-dimensional cell patterns. *Biomed. Microdevices*, **6** (2), 139–147.

23 Hopp, B., Smausz, T., Zs, A., Kresz, N., Zs, B., and Chrisey, D. (2004) Absorbing film assisted laser induced forward transfer of fungi (Trichoderma conidia). *J. Appl. Phys.*, **96** (6), 3478–3481.

24 Hopp, B., Smausz, T., Kresz, N., Barna, N., Bor, Z., Kolozsvári, L., Chrisey, D.B., Szabó, A., and Nógrádi, A. (2005) Survival and proliferative ability of various living cell types after laser-induced forward transfer. *Tissue Eng.*, **11**, 1817–1823.

25 Hopp, B., Smausz, T., Szabo, G., Kolozsvari, L., Kafetzopoulos, D., Fotakis, C., and Nogradi, A. (2013) Femtosecond laser printing of living cells using absorbing film-assisted laser-induced forward transfer. *Opt. Eng.*, **51** (1), 014302.

26 Kattamis, N.T., McDaniel, N.D., Bernhard, S., and Arnold, C.B. (2009) Laser direct write printing of sensitive and robust light emitting organic molecules. *Appl. Phys. Lett.*, **94**, 103306.

27 Kattamis, N.T., Purnick, P.E., Weiss, R., and Arnold, C.B. (2007) Thick film laser induced forward transfer for deposition of thermally and mechanically sensitive materials. *Appl. Phys. Lett.*, **91**, 171120.

28 Fukumura, H., Kohji, Y., Nagasawa, K.-I., and Masuhara, H. (1994) Laser implantation of pyrene molecules into poly(methyl methacrylate) films. *J. Am. Chem. Soc.*, **116** (22), 10304–10305.

29 Mito, T., Tsujita, T., Masuhara, H., Hayashi, N., and Suzuki, K. (2001) Hollowing and transfer of polymethyl methacrylate film propelled by laser ablation of triazeno polymer film. *Jpn. J. Appl. Phys.*, **40** (2-8A), L805–L806.

30 Lippert, T., Wokaun, A., Stebani, J., Nuyken, O., and Ihlemann, J. (1993) Triazene polymers designed for excimer laser ablation. *Angew. Makromol. Chem.*, **206**, 97–110.

31 Stebani, J., Nuyken, O., Lippert, T., and Wokaun, A. (1993) Synthesis and characterization of a novel photosensitive triazene polymer. *Makromol. Chem. Rapid Commun.*, **14**, 365.

32 Lippert, T., Yabe, A., and Wokaun, A. (1997) Laser ablation of doped polymer systems. *Adv. Mater.*, **9** (2), 105–119.

33 Lippert, T., Wei, J., Wokaun, A., Hoogen, N., and Nuyken, O. (2000) Development and structuring of combined positive–negative/negative–positive resists using laser ablation as positive dry etching technique. *Macromol. Mater. Eng.*, **283**, 140–143.

34 Lippert, T., David, C., Dickinson, J.T., Hauer, M., Kogelschatz, U., Langford, S.C., Nuyken, O., Robert, J., and Wokaun, A. (2001) Structure property relations of photoreactive polymers designed for laser ablation. *J. Photochem. Photobiol., A*, **145**, 145–157.

35 Lippert, T. (2009) UV Laser ablation of polymers: from structuring to thin film deposition, in *Laser-Surface Interactions for New Materials Production Tailoring Structure and Properties*, Springer Series in Materials Chemistry, vol. **130** (eds A. Miotello and P.M. Ossi), Springer-Verlag, Berlin, pp. 141–175.

36 Lippert, T. and Dickinson, J.T. (2003) Chemical and spectroscopic aspects of polymer ablation- special features and novel directions. *Chem. Rev.*, **103**, 453–485.

37 Lippert, T., Nakamura, T., Niino, H., and Yabe, A. (1997) Laser induced chemical and physical modifications of polymer films: dependence on the irradiation wavelength. *Appl. Surf. Sci.*, **110**, 227–231.

38 Fardel, R., Nagel, M., Nuesch, F., Lippert, T., and Wokaun, A. (2009) Shadowgraphy investigation of laser-induced forward transfer: front side and back side ablation of the triazene polymer sacrificial layer. *Appl. Surf. Sci.*, **255**, 5430–5434.

39 Fardel, R., Nagel, M., Nuesch, F., Lippert, T., and Wokaun, A. (2007) Laser forward transfer using a sacrificial layer: influence of the material properties. *Appl. Surf. Sci.*, **254**, 1322–1326.

40 Fardel, R., Feurer, P., Lippert, T., Nagel, M., Nuesch, F., and Wokaun, A. (2007) Laser ablation of aryltriazene photopolymer films: effects of polymer structure on ablation properties. *Appl. Surf. Sci.*, **254**, 1332–1337.

41 Hauer, M., Funk, D., Lippert, T., and Wokaun, A. (2003) Laser ablation of polymers studied by ns-interferometry and ns-shadowgraphy measurements. *Appl. Surf. Sci.*, **208–209**, 107–112.

42 Hauer, M., Funk, D., Lippert, T., and Wokaun, A. (2005) Time resolved techniques as probes for the laser ablation process. *Opt. Lasers Eng.*, **43** (3–5), 545–556.

43 Fardel, R., Nagel, M., Nuesch, F., Lippert, T., Wokaun, A., and Luk'yanchuk, B. (2008) Influence of thermal diffusion on the laser ablation of thin polymer films. *Appl. Phys. A*, **90**, 661–667.

44 Fardel, R., Nagel, M., Nuesch, F., Lippert, T., and Wokaun, A. (2009) Energy balance in a laser-induced forward transfer process studied by shadowgraphy. *J. Phys. Chem. C*, **113**, 11628–11633.

45 Rapp, L., Cibert, C., Nenon, S., Alloncle, A.P., Nagel, M., Lippert, T., Videlot-Ackermann, C., Fages, F., and Delaporte, P. (2011) Improvement in semiconductor laser printing using a sacrificial protecting layer for organic thin-film transistors fabrication. *Appl. Surf. Sci.*, **257**, 5245–5249.

46 Nagel, M. and Lippert, T. (2012) Laser-Induced Forward Transfer for the fabrication of devices, in *Nanomaterials: Processing and Characterization with Lasers* (eds S.C. Singh, H. Zeng, C. Guo, and C. Weiping), Wiley-VCH Verlag GmBH, pp. 255–316.

47 Doraiswamy, A., Narayan, R., Lippert, T., Urech, L., Wokaun, A., Nagel, M., Hopp, B., Dinescu, M., Modi, R., Auyeung, R., and Chrisey, D. (2006) Excimer laser forward transfer of mammalian cells using a novel triazene absorbing layer. *Appl. Surf. Sci.*, **252**, 4743–4747.

48 Xu, J., Liu, J., Cui, D., Gerhold, M., Wang, A., Nagel, M., and Lippert, T. (2007) Laser-assisted forward transfer of multi-spectral nanocrystal quantum dot emitters. *Nanotechnology*, **18**, 025403.

49 Palla-Papavlu, A., Paraico, I., Shaw-Stewart, J., Dinca, V., Savopol, T., Kovacs, E., Lippert, T., Wokaun, A., and Dinescu, M. (2011) Liposome micropatterning based on laser-induced forward transfer. *Appl. Phys. A Mater. Sci. Process.*, **102** (3), 651–659.

50 Banks, D., Kaur, K., Gazia, R., Fardel, R., Nagel, M., Lippert, T., and Eason, R. (2008) Triazene photopolymer dynamic release layer-assisted femtosecond laser-induced forward transfer with an active carrier substrate. *EPL (Europhys. Lett.)*, **83**, 38003.

51 Mattle, T., Shaw-Stewart, J., Schneider, C.W., Lippert, T., and Wokaun, A. (2012) Laser induced forward transfer aluminum layers: process investigation by time resolved imaging. *Appl. Surf. Sci.*, **258**, 9352–9354.

52 Dinca, V., Palla-Papavlu, A., Dinescu, M., Shaw-Stewart, J., Lippert, T., Di Pietrantonio, F., Cannata, D., Benetti, M., and Verona, E. (2010) Polymer pixel enhancement by laser-induced forward transfer for sensor applications. *Appl. Phys. A*, **101**, 559–565.

53 Dinca, V., Palla-Papavlu, A., Matei, A., Luculescu, C., Dinescu, M., Lippert, T., Di Pietrantonio, F., Cannata, D., Benetti, M., and Verona, E. (2010) A comparative study of DRL-lift and lift on integrated polyisobutylene polymer matrices. *Appl. Phys. A*, **101**, 429–434.

54 Di Pietrantonio, F., Benetti, M., Cannata, D., Verona, E., Palla-Papavlu, A., Dinca, V., Dinescu, M., Mattle, T., and Lippert, T. (2012) Volatile toxic compound detection by surface acoustic wave sensor array coated with chemoselective polymers deposited by laser induced forward transfer: application to sarin. *Sens. Actuators, B*, **174**, 158–167.

55 Cannata, D., Benetti, M., Di Pietrantonio, F., Verona, E., Palla-Papavlu, A., Dinca, V., Dinescu, M., and Lippert, T. (2012) Nerve agent simulant detection by solidly mounted resonators (SMRs) polymer coated using laser induced forward transfer (LIFT) technique. *Sens. Actuators, B*, **173**, 32–39.

56 Dinca, V., Mattle, T., Palla-Papavlu, A., Rusen, L., Luculescu, C., Lippert, T., and Dinescu, M. (2013) Polyethyleneimine patterns obtained by laser-transfer assisted by a Dynamic Release Layer onto Themanox soft substrates for cell adhesion study. *Appl. Surf. Sci.*, **278**, 190–197.

57 Inui, T., Mandamparambil, R., Araki, T., Abbel, R., Koga, H., Nogia, M., and Suganuma, K. (2015) Laser-induced forward transfer of high-viscosity silver precursor ink for non-contact printed electronics. *RSC Adv.*, **5**, 77942–77947.

58 Palla-Papavlu, A., Dinca, V., Paraico, I., Moldovan, A., Shaw-Stewart, J., Schneider, C.W., Kovacs, E., Lippert, T., and Dinescu, M. (2010) Microfabrication of polystyrene microbead arrays by laser induced forward transfer. *J. Appl. Phys.*, **108**, 033111–033116.

59 Palla-Papavlu, A., Dinca, V., Luculescu, C., Shaw-Stewart, J., Nagel, M., and Dinescu, M. (2010) Laser induced forward transfer of soft materials. *J. Opt.*, **12**, 124114–124119.

60 Palla-Papavlu, A., Dinescu, M., Wokaun, A., and Lippert, T. (2014) Laser-induced forward transfer of single-walled carbon nanotubes. *Appl. Phys. A*, **117**, 371–376.

61 Rapp, L., Diallo, A.K., Nénon, S., Alloncle, A.P., Videlot-Ackermann, C., Fages, F., Nagel, M., Lippert, T., and Delaporte, P. (2012) Laser printing of a semiconducting oligomer as active layer in organic thin film transistors: Impact of a protecting triazene layer. *Thin Solid Films*, **520**, 3043–3047.

62 Chen, J., Palla-Papavlu, A., Li, Y., Chen, L., Dobeli, M., Stender, D., Populoh, S., Weidenkaff, A., Schenider, C.W., Wokaun, A., and Lippert, T. (2014) Laser direct deposition and direct-writing of thermoelectric misfit cobaltite thin films. *Appl. Phys. Lett.*, **104**, 231907.

63 Fardel, R., Nagel, M., Nüesch, F., Lippert, T., and Wokaun, A. (2007) Fabrication of organic light-emitting diode pixels by laser-assisted forward transfer. *Appl. Phys. Lett.*, **91**, 061103.

64 Shaw-Stewart, J., Lippert, T., Nagel, M., Nuesch, F., and Wokaun, A. (2011) Laser-induced forward transfer of polymer light-emitting pixels with increased charge injection. *ACS Appl. Mater. Interfaces*, **3**, 309–316.

65 Shaw-Stewart, J., Lippert, T., Nagel, M., Nuesch, F., and Wokaun, A. (2012) Sequential printing by laser-induced forward transfer to fabricate a polymer light-emitting diode pixel. *ACS Appl. Mater. Interfaces*, **4**, 3535–3541.

66 Mattle, T., Hintennach, A., Lippert, T., and Wokaun, A. (2013) Laser induced forward transfer of SnO_2 for sensing applications using different precursors systems. *Appl. Phys. A*, **110**, 309–316.

67 Palla-Papavlu, A., Mattle, T., Temmel, S., Lehmann, U., Hintennach, A., Grisel, A., Wokaun, A., and Lippert, T. (2016) Highly sensitive SnO_2 sensor via reactive laser-induced transfer. *Sci. Rep.*, **6**, 25144.

68 Shaw-Stewart J., Lippert T., Nagel M., Nuesch F., and Wokaun A. (2010) Laser-induced forward transfer using Triazene polymer dynamic releaser layer. AIP Conference Proceedings, vol. 1278, pp. 789–799.

69 Shaw-Stewart, J.R.H. (2012) Optimizing the fabrication of organic light-emitting diodes by laser-induced forward transfer. PhD thesis. ETH.

70 Ballantine, D.S., White, R.M., Martin, S.J., Ricco, A.J., Frye, G.C., Zellers, E.T., and Wohltjen, H. (1997) *Acoustic Wave Sensors: Theory, Design, and Physico-Chemical Applications*, John Wiley & Sons, Inc., New York, ISBN: 978-0-12-077460-9.

71 Martin, S.J., Frye, G.C., Spates, J.J., and Butler, M.A. (1996) Gas sensing with acoustic devices. Proceedings of IEEE Ultrasonics Symposium, vol. 421, pp. 423–434.

72 Dinescu, M., Matei, A., Dinca, V., Palla-Papavlu, A., Di Pietrantonio, F., Cannata, D., Benetti, M., Verona, E., and Lippert, T. (2013) Laser processing of organic materials: applications in tissue engineering and chemical sensing. *Rom. Rep. Phys.*, **65** (3), 1019–1031.

73 Ballantine, D.S., Rose, S.L., Grate, J.W., and Wohltjen, H. (1986) Correlation of surface acoustic wave device coating responses with solubility properties and chemical structure using pattern recognition. *Anal. Chem.*, **58** (14), 3058–3066.

74 Rose-Pehrsson, S.L., Grate, J.W., Ballantine, D.S., and Jurs, P.C. (1988) Detection of hazardous vapors including mixtures using pattern recognition analysis of responses from surface acoustic wave devices. *Anal. Chem.*, **60**, 2801–2811.

75 Kaur, K.S., Feinaeugle, M., Banks, D.P., Ou, J.Y., Di Pietrantonio, F., Verona, E., Sones, C.L., and Eason, R.W. (2011) Laser-induced forward transfer of focused ion beam pre-machined donors. *Appl. Surf. Sci.*, **257** (15), 6650–6653.

76 Palla-Papavlu, A., Constantinescu, C., Dinca, V., Matei, A., Moldovan, A., Mitu, B., and Dinescu, M. (2010) Polyisobutylene thin films obtained by matrix assisted pulsed laser evaporation for sensors applications. *Sens. Lett.*, **8** (3), 502–506.

77 Pinna, N., Garnweitner, G., Antonietti, M., and Niederberger, M. (2005) A general nonaqueous route to binary metal oxide nanocrystals involving a C-C bond cleavage. *J. Am. Chem. Soc.*, **127** (15), 5608–5612.
78 Niederberger, M., Garnweitner, G., Krumeich, F., Nesper, R., Colfen, H., and Antonietti, M. (2004) Tailoring the surface and solubility properties of nanocrystalline titania by a nonaqueous in situ functionalization process. *Chem. Mater.*, **16** (7), 1202–1208.
79 Wu, J.M., Chen, Y.-R., and Kao, W.T. (2014) Ultrafine ZnO nanoparticles/nanowires synthesized on a flexible and transparent substrate: formation, water molecules, and surface defect effects. *ACS Appl. Mater. Interfaces*, **6**, 487–494.
80 Benetti, M., Cannata, D., D'Amico, A., Di Pietrantonio, F., Macagnano, A., and Verona, E. (2004) SAW sensors on AlN/diamond/Si structures. Proceedings of IEEE Sensors, vol. 752, pp. 753–756.